Scientific Reports

https://doi.org/10.1038/s41598-026-35349-0

Article in Press

Fuel cell PV fed hybrid energy sources for 3 phase matrix converter using 3D Space Vector Modulation

Received: 4 August 2025

Accepted: 5 January 2026

Published online: 25 February 2026

Cite this article as: Palanisamy R., Thentral T.M.T., Usha S. *et al.* Fuel cell PV fed hybrid energy sources for 3 phase matrix converter using 3D Space Vector Modulation. *Sci Rep* (2026). https://doi.org/10.1038/s41598-026-35349-0

R. Palanisamy, T. M. Thamizh Thentral, S. Usha, A. Geetha, C. Ahamed Saleel, Parvathy Rajendran, It Ee Lee & Fayaz Hussain

Fuel Cell PV Fed Hybrid Energy Sources for 3 Phase Matrix Converter using 3D Space Vector Modulation

Palanisamy R [1]*, Thamizh Thentral TM [1], Usha S [1], Geetha A [1], C Ahamed Saleel [2,3], Parvathy Rajendran [4]*, It Ee Lee [5,6]*, Fayaz Hussain [7]*

[1]Department of Electrical and Electronics Engineering, SRM Institute of Science and Technology, Kattankulathur, Chennai, Tamilnadu, India -603203. palanisr@srmist.edu.in; *thamizht@srmist.edu.in; ushas@srmist.edu.in; geethaa2@srmist.edu.in*

[2]Department of Mechanical Engineering, College of Engineering, King Khalid University, PO Box 394, Abha 61421, Saudi Arabia; ahamedsaleel@gmail.com

[3]Center for Engineering and Technology Innovations, King Khalid University, Abha 61421, Saudi Arabia

[4] Department of Mechanical and Aerospace Engineering, United Arab Emirates University, Al Ain, UAE

[5]Faculty of Artificial Intelligence and Engineering, Multimedia University, 63100 Cyberjaya, Malaysia

[6]Centre for Smart Systems and Automation, COE for Robotics and Sensing Technologies, Multimedia University, 63100 Cyberjaya, Malaysia

[7] Department of Biological and Agricultural Engineering, Faculty of Engineering, Universiti Putra Malaysia, Selangor, Malaysia.
fayazhussain@upm.edu.my

Corresponding author: palanisr@srmist.edu.in; ielee@mmu.edu.my, aeparvathy@uaeu.ac.ae ; fayazhussain@upm.edu.my

Abstract

The increasing global demand for clean and sustainable energy has driven the integration of renewable energy sources with advanced power electronic converters. This paper presents a novel hybrid energy system combining Proton Exchange Membrane Fuel Cell (PEMFC) and

Photovoltaic (PV) sources to feed a three-phase matrix converter (MC), employing a 3D Space Vector Modulation (3D-SVM) strategy. The hybrid configuration ensures a stable and continuous power supply, overcoming the intermittency of solar energy and the slow dynamic response of fuel cells. The 3-phase matrix converter, recognized for its bidirectional power flow, compact structure, and high-quality output, is controlled using the 3D-SVM technique to achieve improved voltage transfer ratio, minimized Total Harmonic Distortion (THD), reduced Common Mode Voltage (CMV), less neutral current, and enhanced dynamic performance. The proposed modulation strategy optimally synthesizes switching state vectors in 3D-cubic region, ensuring effective real-time control and power management of the hybrid energy system. The simulation and hardware results of the proposed system validates the performance of 3-phase matrix converter with hybrid energy sources.

Keywords: Fuel Cell, Photovoltaic (PV), Hybrid Energy System, Matrix Converter, 3D Space Vector Modulation (3D-SVM), Renewable Energy Integration, Total Harmonic Distortion (THD).

1. Introduction

The global transition toward sustainable and renewable energy has led to the advancement of hybrid energy systems that merge multiple clean energy sources to meet varying power demands efficiently and reliably [1]-[2]. Among the numerous renewable sources, PEMFC and Photovoltaic systems have gained considerable attention due to their complementary characteristics [3]-[4]. PV systems offer clean and free energy from sunlight, while fuel cells provide stable and continuous power with high efficiency and low emissions [6]. However, both systems also have inherent limitations. PV systems suffer from intermittency due to weather and sunlight availability, while fuel cells have slower dynamic response and high initial costs. Combining these sources into a hybrid configuration

allows for a more resilient energy system that can supply uninterrupted power in varying environmental conditions [7].

In hybrid systems, the choice of power conversion technology plays a critical role in maintaining the quality, efficiency, and reliability of the energy supplied [8]. Traditional power conversion methods often involve multiple stages with bulky passive components, leading to reduced system efficiency and increased footprint. To address these challenges, matrix converters have emerged as a promising alternative [9]. A matrix converter is a direct AC-to-AC converter that reduces the need for transitional DC links and energy storage elements [10]. It offers benefits such as reduced size and weight, bidirectional power flow capability, and improved output waveform quality [11]. These features make the matrix converter an attractive option for interfacing renewable energy sources with AC loads or the grid, especially in applications where space and efficiency are crucial [12].

MPPT is a vital control strategy used in photovoltaic energy systems to consistently harvest the highest possible power output, even as environmental factors like irradiance and temperature change [13]. Conventional MPPT approaches work by adjusting the PV system's operating conditions to coincide with the maximum power point, thus optimizing energy conversion efficiency. [14]. However, conventional algorithms often struggle with tracking accuracy and speed, especially under rapidly changing conditions. To address these challenges, fuzzy logic-based MPPT methods have been introduced, offering a more adaptive and intelligent approach [15]. By employing a set of linguistic rules and fuzzy inference, fuzzy-based MPPT can effectively handle nonlinearity and uncertainties without demanding an precise mathematical model of the PV system [16]. This results in improved tracking performance, faster response, and greater robustness compared to traditional methods.

Inverters play a vital role in modern electrical and renewable energy systems by converting direct current into alternating current to meet the requirements of various applications such as grid integration, industrial

drives, and domestic power supply [17]. Among different inverter types, VSIs are widely preferred due to their ability to maintain a constant voltage at the output regardless of load variations. VSI-based systems offer advantages such as simple control strategies, fast dynamic response, and compatibility with renewable sources like photovoltaic and wind energy systems [18]. The need for efficient, reliable, and high-performance inverters has increased significantly with the growing emphasis on sustainable energy and smart grid technologies, positioning VSI as a fundamental building block in advanced power electronic applications [19].

The control of matrix converters is a complex task due to the large number of switching states and the need to maintain input-output voltage and current relationships within safe limits [20]. To achieve effective control, various modulation strategies have been developed, among which Space Vector Modulation has proven to be one of the most efficient and widely used. method plays a crucial role in modern power electronics, particularly in the control of voltage source inverters and matrix converters [21]. Its importance stems from its ability to produce high-quality output waveforms, maximize the DC bus voltage utilization, and reduce harmonic distortion. The conventional two-dimensional SVM is effective for standard voltage source inverters, but when applied to matrix converters, especially in three-phase systems, it becomes necessary to use a more advanced technique such as 3D-SVM [22]. 3D-SVM extends the traditional approach by considering the full three-dimensional space of input and output vectors, enabling more precise control over the switching states.

The implementation of 3D-SVM in matrix converters provides several performance advantages, including higher voltage transfer ratios, better harmonic performance, and improved dynamic response under varying load conditions [23]. These improvements are critical in hybrid renewable energy systems where the input conditions can vary significantly [24]. The 3D-SVM technique ensures that the hybrid fuel cell-

PV energy system can deliver stable and high-quality AC power, meeting the demands of modern electrical loads while minimizing losses and total harmonic distortions.

Hybrid renewable energy systems combining photovoltaic (PV) and fuel cell technologies have attracted significant attention due to their complementary characteristics: PV systems offer clean and low-cost generation, while Proton Exchange Membrane Fuel Cells (PEMFCs) provide stable power backup with high efficiency and low emissions. Early work on PV–fuel cell hybrids focused primarily on energy balance and sizing optimization [25]. For instance, demonstrated a PV–fuel cell system with battery storage for standalone applications, highlighting the improved reliability compared to standalone PV systems. However, such studies did not emphasize power quality improvement or advanced converter control strategies.

In order to interface hybrid energy sources with AC loads or grids, power electronic converters play a pivotal role. Conventional approaches typically employ DC–DC converters for each source followed by a voltage source inverter (VSI) to generate AC outputs [26]. Multilevel converters such as neutral-point-clamped (NPC), flying capacitor (FC), and cascaded H-bridge topologies have been widely used due to their ability to produce high-quality voltage waveforms with reduced harmonic distortion and improved efficiency. For example, Zhao et al. implemented a three-level NPC converter with PWM modulation in a PV–fuel cell hybrid system, reporting significant THD reduction and enhanced DC–link stability.

Despite the advantages of multilevel converters, they inherently require large passive components and energy storage elements (e.g., capacitors and inductors), which increase system size, cost, and maintenance requirements [27]. Moreover, achieving bidirectional power flow and seamless power sharing between multiple sources is nontrivial with traditional multilevel VSI structures. To address these limitations, matrix converters (MCs) have emerged as an attractive alternative. Unlike traditional AC–DC–AC conversion chains, MCs provide direct AC–AC

conversion without an intermediate DC-link, eliminating bulky DC capacitors and enhancing power density and reliability.

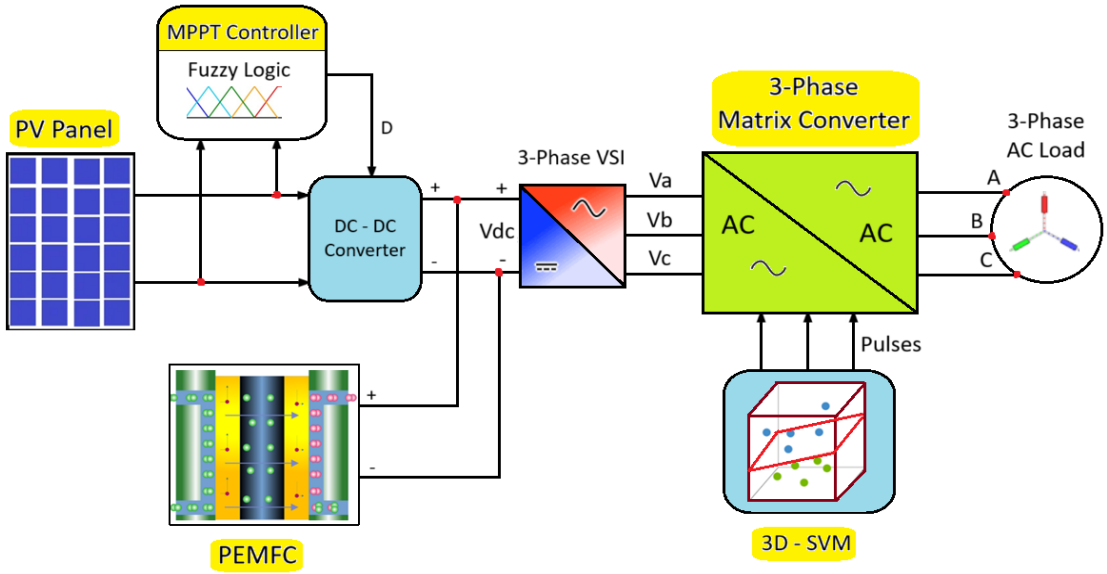

Fig.1. Schematic diagram of proposed hybrid energy for 3-Phase Matrix Converter using 3D-SVM

This research focuses on the integration of PEMFC and PV sources into a hybrid energy system that feeds a three-phase matrix converter controlled using 3D-SVM. The primary objectives are to design a system that maximizes the utilization of available renewable resources, ensures seamless power delivery, and maintains high power quality standards. The study includes system modeling, control strategy development, simulation, and performance analysis under various operating scenarios. The results are expected to demonstrate the feasibility and effectiveness of using advanced modulation techniques like 3D-SVM in enhancing the performance of hybrid energy systems involving matrix converters.

2. Hybrid Energy Source – PV and PEMFC

Hybrid energy systems combining Photovoltaic and Proton Exchange Membrane Fuel Cell offer a promising solution to address the limitations of individual renewable sources while enhancing energy reliability, efficiency, and sustainability [28]. PV systems are

environmentally friendly and capable of generating electricity directly from solar radiation, but their output is inherently intermittent and weather dependent. PEMFCs, on the other hand, provide stable and continuous power with high efficiency and low emissions, though they are less responsive to rapid load variations and require hydrogen fuel [29]. By integrating these two sources, the hybrid system leverages the clean, renewable nature of solar energy and the steady power supply of fuel cells, resulting in a complementary energy profile ideal for uninterrupted and resilient power delivery [30]. This combination is particularly suited for applications in smart grids, distributed generation, and remote or off-grid locations, where energy reliability and quality are critical.

2.1 PV System

The modeling of a Photovoltaic (PV) system is a fundamental step in the design, analysis, and optimization of solar energy applications. A PV system converts solar radiation directly into electrical energy using semiconductor materials, typically silicon-based solar cells. Accurate modeling of the PV system involves understanding the electrical behavior of the solar cell under varying environmental conditions such as irradiance and temperature. The most used model for this purpose is the single-diode equivalent circuit is shown in fig.2a, which includes a current source, freewheel diode, series and shunt resistance to simulate the real behavior of a solar cell.

This model helps predict the output characteristics such as current-voltage is shown in fig.2b and power-voltage curves is shown in fig.3a, which are essential for system design and maximum power point tracking (MPPT). Additionally, PV system modeling includes considerations for module configuration, inverter integration, partial shading effects, and dynamic response under real-time conditions. Accurate and dynamic PV modeling is crucial for ensuring efficient energy harvesting, system reliability, and effective control in standalone or grid-connected hybrid renewable energy systems.

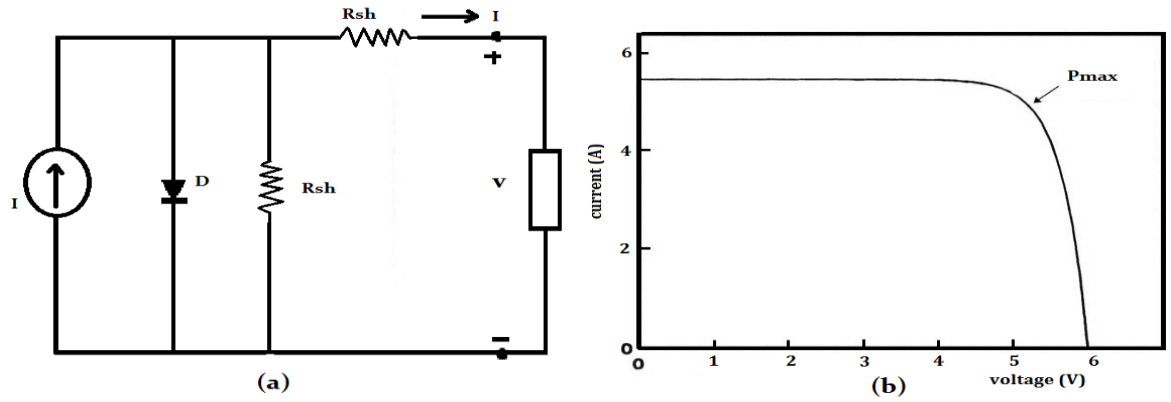

Fig. 2. PV structure a) equivalent circuit b) IV characteristics

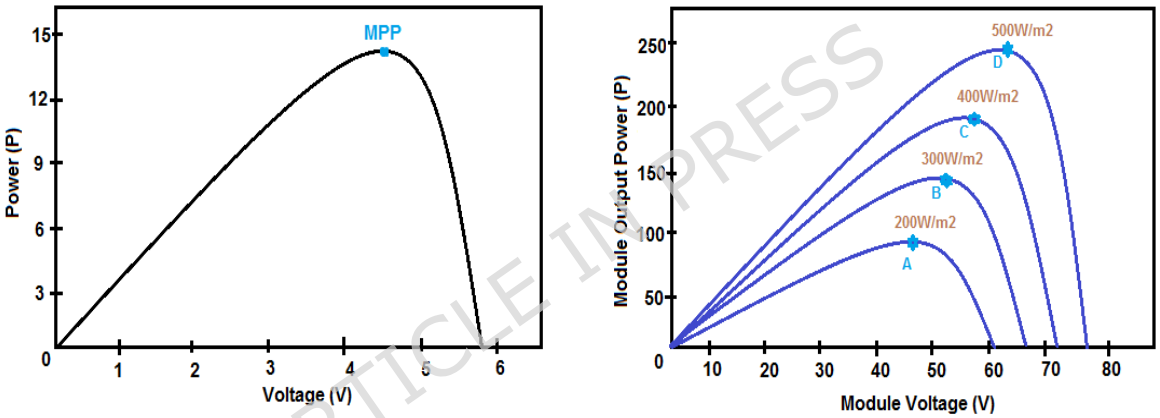

Fig.3 a) P-Vi characteristics of cell b) Fuzzy based MPPT with varying irradiance

2.2. Fuzzy based MPPT controller

In the proposed hybrid energy system comprising a photovoltaic (PV) array and a proton-exchange membrane fuel cell (PEMFC), the PV subsystem is integrated with a Fuzzy Logic Controller (FLC)-based Maximum Power Point Tracking strategy to ensure efficient solar energy extraction under varying atmospheric conditions. Unlike conventional MPPT methods such as Perturb and Observe or Incremental Conductance, the fuzzy-based MPPT does not rely on a detailed mathematical model and exhibits

superior dynamic response and robustness. The controller uses the slope of the power-voltage (P-V) curve and its rate of change as inputs to determine the optimal duty cycle for a boost converter, thereby dynamically regulating the operating point of the PV array. A rule-based decision framework with fuzzy inference ensures smooth and accurate convergence to the Maximum Power Point (MPP), even in scenarios involving rapid changes in irradiance or partial shading.

The regulated DC power from the PV unit, alongside the output from the fuel cell, forms a hybrid DC link that feeds a three-phase matrix converter controlled by 3D-SVM. The fuzzy MPPT ensures that the PV system consistently contributes maximum power to the shared DC link, thereby reducing the burden on the fuel cell and improving overall system efficiency. This approach enables effective power sharing and voltage stabilization, which is critical for matrix converters that lack intermediate energy storage elements. Additionally, the adaptive nature of the FLC enhances system resilience, making it ideal for smart grid and distributed generation applications where environmental variability is a key challenge. Fuzzy error membership functions and error rate membership function is shown in fig 4a & 4b respectively.

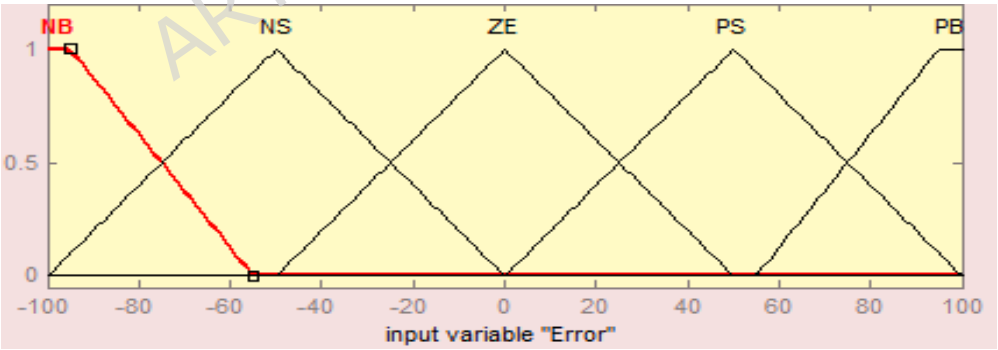

(a)

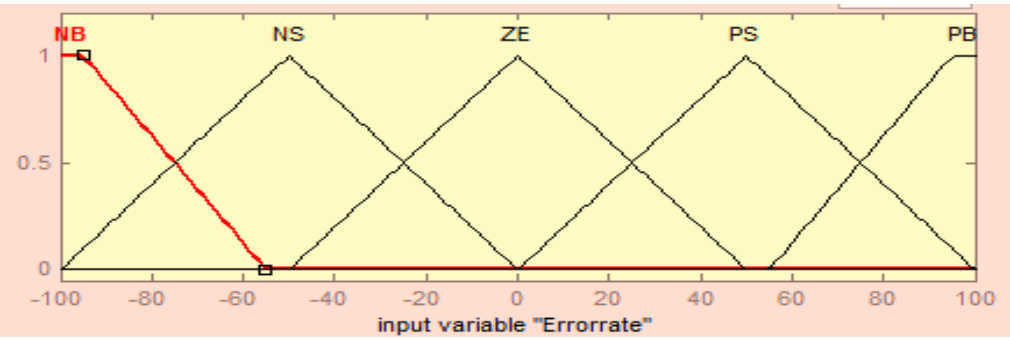

(b)

Fig. 4. Fuzzy MPPT control (a) error membership functions (b) error rete membership function

Table. 1. Fuzzy Rules used for MPPT controller

Error (E) \ (ΔE)	NB	NM	NS	ZE	PS	PM	PB
NB	NB	NB	NM	NM	NS	ZE	ZE
NM	NB	NM	NM	NS	ZE	PS	PS
NS	NM	NM	NS	ZE	PS	PM	PM
ZE	NM	NS	ZE	ZE	ZE	PS	PM
PS	NS	ZE	PS	PS	PM	PM	PB
PM	ZE	PS	PM	PM	PB	PB	PB
PB	ZE	PM	PM	PB	PB	PB	PB

The fuzzy rule base in table.1 governs the control logic for adjusting the duty cycle of the DC-DC converter connected to the PV panel, thereby guiding the system towards the Maximum Power Point (MPP). The table entries are based on two inputs: Error (E) and Change in Error (ΔE). Error (E) = ΔP/ΔV: Represents the slope of the PV power-voltage curve. In a PV system, the slope of the power-voltage curve, represented as ΔP/ΔV, is a key indicator for determining the operating point relative to the MPP. A positive slope indicates that the system is operating to the left of MPP, meaning the voltage is too low and increasing it will lead to more power extraction. A negative slope means the system is to the right of MPP, where the voltage is too high and needs to be reduced to reach maximum power.

When the slope is zero, the system is precisely at the MPP, and no further adjustment to the voltage or duty cycle is necessary. This slope behavior is fundamental in guiding MPPT algorithms, especially intelligent ones like Fuzzy Logic Controllers, to continuously track and maintain the PV system at its most efficient operating point. The ΔE value indicates how the slope is changing with time, i.e., whether the system is advancing or stepping away from MPP.

The fuzzy rule base table is to provide a structured and adaptive control mechanism that enables efficient tracking of the MPP in a PV system. Its symmetric structure ensures balanced decision-making and smooth transitions across various operating conditions, minimizing sudden changes that could destabilize the system. This design helps the MPPT controller avoid unnecessary oscillations around the MPP, maintaining steady performance even under fluctuating irradiance and temperature. Additionally, the rapid response capability of the fuzzy controller allows for fast tracking during dynamic environmental changes, ensuring that the PV array consistently operates near its optimal point. This not only maximizes solar energy utilization but also improves the overall performance of the hybrid PV-Fuel Cell system by reducing the load demand on the fuel cell, enhancing system efficiency and reliability.

2.3 PEMFC

A PEMFC is an electrochemical system that directly transforms the chemical energy from hydrogen and oxygen into electricity, producing only water and heat as byproducts. Thanks to their low operating temperatures, rapid start-up capabilities, high power density, and environmentally friendly emissions, PEMFCs are particularly well-suited for portable, automotive, and stationary power applications. Their core advantage lies in their ability to deliver efficient and environmentally friendly power, making them an ideal candidate for integration into renewable hybrid energy systems such as PV-Fuel Cell configurations.

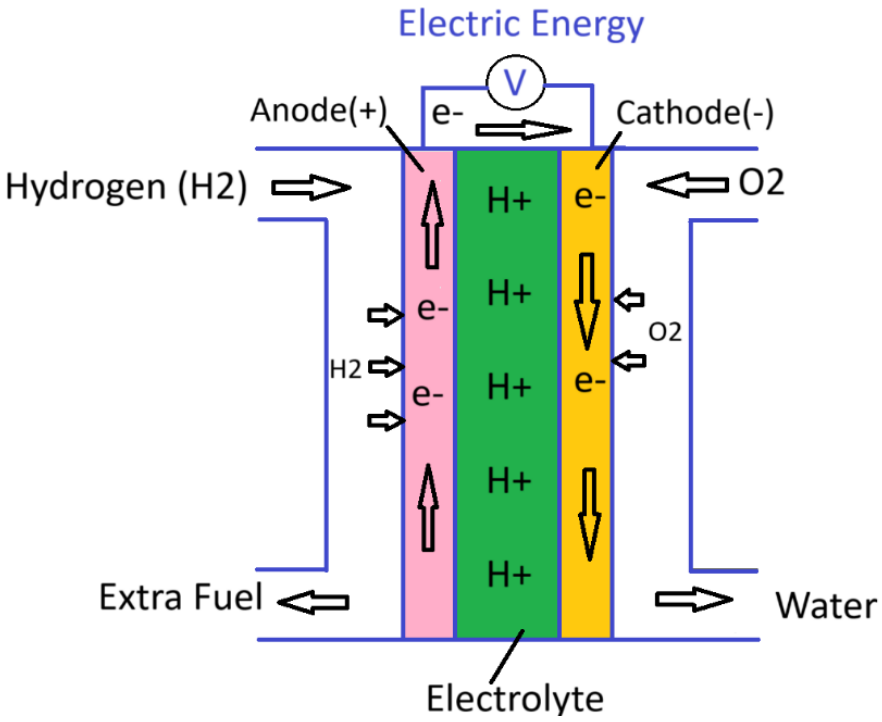

Fig.4. Schematic structure of PEMFC operation

A PEMFC is composed of an anode, a cathode, and a solid polymer electrolyte membrane. Hydrogen gas is fed to the anode, where it is catalytically separated into protons and electrons. While the protons migrate through the proton-conducting membrane to the cathode, the electrons flow through an external circuit, producing an electric current. At the cathode, oxygen gas combines with the arriving protons and electrons to generate water (H_2O) as the sole byproduct. The overall chemical reaction is:

$$2H_2 + O_2 = 2H_2O + \text{Electric Energy} + \text{Extra fuel \& Heat} \quad (1)$$

This clean and efficient process, with zero carbon emissions, makes PEMFC a key technology in sustainable energy systems.

The output voltage of a PEM fuel cell is obtained by subtracting the irreversible losses from the reversible thermodynamic voltage.

$$V_{cell} = E_{Nernst} - V_{act} - V_{ohm} - V_{conc} \quad (2)$$

For a stack of Ncells:

$$V_{stack} = N V_{cell} \quad (3)$$

Reversible (Nernst) Voltage

$$E_{Nernst} = 1.229 - 0.85 \times 10^{-3}(T - 298.15) + \frac{RT}{2F}\ln\left(P_{H_2}\sqrt{P_{O_2}}\right) \quad (4)$$

Activation Losses

$$V_{act} = \frac{RT}{\alpha F}\ln\left(\frac{I}{I_0}\right) \quad (5)$$

Ohmic Losses

$$V_{ohm} = I R_{ohm}$$
$$R_{ohm} = \frac{t_m}{\sigma_m A} \qquad \sigma_m = (0.005139\lambda - 0.00326)\exp\left[1268\left(\frac{1}{303} - \frac{1}{T}\right)\right] \quad (6)$$

Concentration Losses

$$V_{conc} = -\frac{RT}{nF}\ln\left(1 - \frac{I}{I_{lim}}\right) \quad (7)$$

Power and Efficiency

$$P = V_{stack} I$$
$$\eta = \frac{V_{cell}}{1.48}$$

Final Compact PEMFC Voltage Equation

$$V_{stack} = N\left[E_{Nernst} - \frac{RT}{\alpha F}\ln\left(\frac{I}{I_0}\right) - I R_{ohm} - \frac{RT}{nF}\ln\left(1 - \frac{I}{I_{lim}}\right)\right] \quad (8)$$

T - temperature (K), I - stack current (A), F - Faraday constant, R - gas constant, □□$_2$ - partial pressures, I_0 - exchange current, I_{lim} - limiting current.

3. 3-Phase Matrix converter

The fig.5 shown is a 3-phase direct AC-AC matrix converter, which enables the conversion of a 3-phase input AC voltage (a, b, c) directly into

a 3-phase output AC voltage (A, B, C) without using any intermediate DC link. It comprises nine bidirectional switches (S11 to S33) arranged in a 3×3 matrix structure. The converter features three input phases (a, b, c) and three output phases (A, B, C). Each output phase is linked to all three input phases through a set of bidirectional switches. Specifically, output phase A is connected to input phases a, b, and c via switches S11, S21, and S31, respectively.

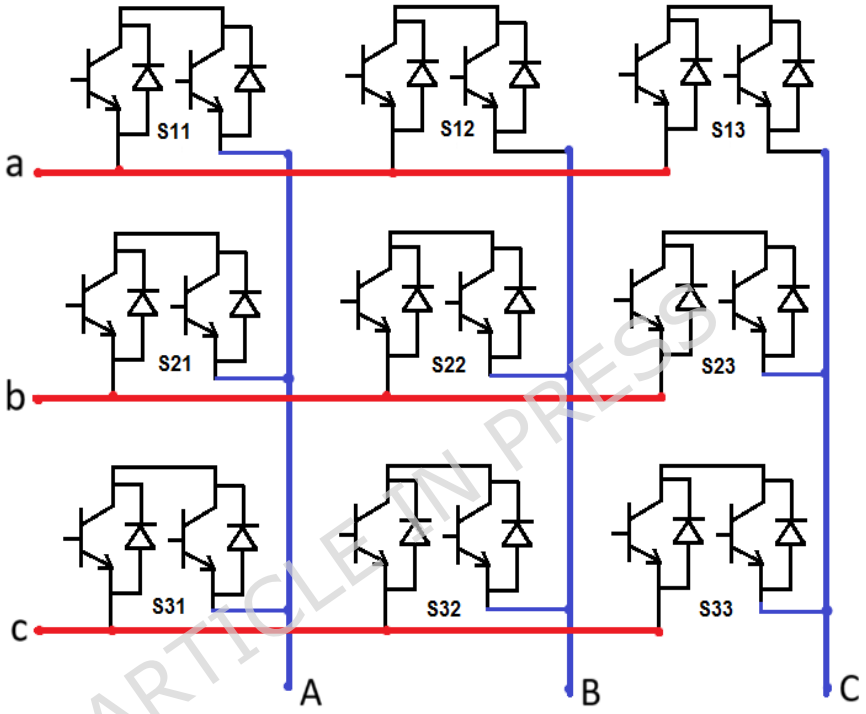

Fig.5. Circuit of 3-phase direct AC-AC matrix converter

Likewise, output phase B connects to inputs a, b, and c through switches S12, S22, and S32, while output phase C is linked to the inputs via switches S13, S23, and S33. Each bidirectional switch is typically made using two IGBTs or MOSFETs in anti-parallel with a freewheeling diode to allow current flow in both directions. In typical power converters, energy storage elements such as capacitors or inductors are used to manage the difference between input and output power. However, with a setup of nine switches (S11 to S33), any output phase can be dynamically linked to any input phase, allowing for flexible power management. However, a matrix converter eliminates the need for such intermediate energy storage by

employing a single-stage power conversion architecture using bidirectional switches. n the absence of energy storage components and under the assumption of ideal, lossless switching, the matrix converter guarantees that instantaneous input power matches the output power, allowing for compact and efficient AC-AC conversion without requiring a transitional DC link.

The three-phase matrix converter directly transforms fixed-frequency AC inputs phases a, b, c into variable-frequency, variable-voltage AC outputs phases A, B, C through a network of nine bidirectional switches organized in a 3×3 matrix configuration. Each output phase is selectively linked to one of the three input phases through appropriate switching actions. At any given moment, each output line is connected to a single input line via a bidirectional switch. The switching sequence is controlled using advanced modulation strategies like 3D Space Vector Modulation, which synthesizes the desired output voltage by adjusting the duty cycles of the switches. This method allows the converter to produce a sinusoidal output voltage and current waveform with a controllable magnitude & frequency, without needing an intermediate DC stage. The result is efficient, compact, and flexible AC-AC power conversion ideal for applications like motor drives and hybrid renewable systems.

The input (V_i) and output (V_0) voltages of 3-phase direct AC to AC matrix converter includes,

$$V_i = \begin{bmatrix} V_a \\ V_b \\ V_c \end{bmatrix} \quad \text{and} \quad V_0 = \begin{bmatrix} V_A \\ V_B \\ V_C \end{bmatrix} \tag{9}$$

Due to the absence of a DC-link capacitor, the matrix converter performs instantaneous power transfer from the source to the load. This enables the formulation of a direct transfer function that links the electrical parameters of the input side with those of the output side. Based on this principle, the output voltage vector can be expressed as a function of the input voltage vector through an instantaneous transfer matrix is,

$$\begin{bmatrix} V_A \\ V_B \\ V_C \end{bmatrix} = \begin{bmatrix} S_{11} & S_{21} & S_{31} \\ S_{12} & S_{22} & S_{32} \\ S_{13} & S_{23} & S_{33} \end{bmatrix} \begin{bmatrix} V_a \\ V_b \\ V_c \end{bmatrix}$$

(10)

The above 3-phase direct AC to AC conversion output voltage is rewritten as,

$$V_0 = M(S_{nM)} V_i$$

(11)

Where S_{nM}represents 3*3 matrix conversion; n-input voltage & M – output voltage.

Here, $M(S_{nM)}$ is the instantaneous transfer matrix, which reflects the current switching state of the converter. Each row in the matrix corresponds to the switches associated with a specific output phase, while each column corresponds to the switches associated with a specific input phase. This matrix serves as the foundation for implementing advanced modulation schemes, such as space vector modulation, for precise control of the matrix converter.

The same concept used to calculate load current of 3-phase direct AC to AC matrix converter. The load current is defined as,

$$\begin{bmatrix} I_A \\ I_B \\ I_C \end{bmatrix} = \begin{bmatrix} S_{11} & S_{21} & S_{31} \\ S_{12} & S_{22} & S_{32} \\ S_{13} & S_{23} & S_{33} \end{bmatrix} \begin{bmatrix} I_a \\ I_b \\ I_c \end{bmatrix}$$

(12)

The above 3-phase direct AC to AC conversion output load current is,

$$I_0 = M(S_{nM)} I_i$$

(13)

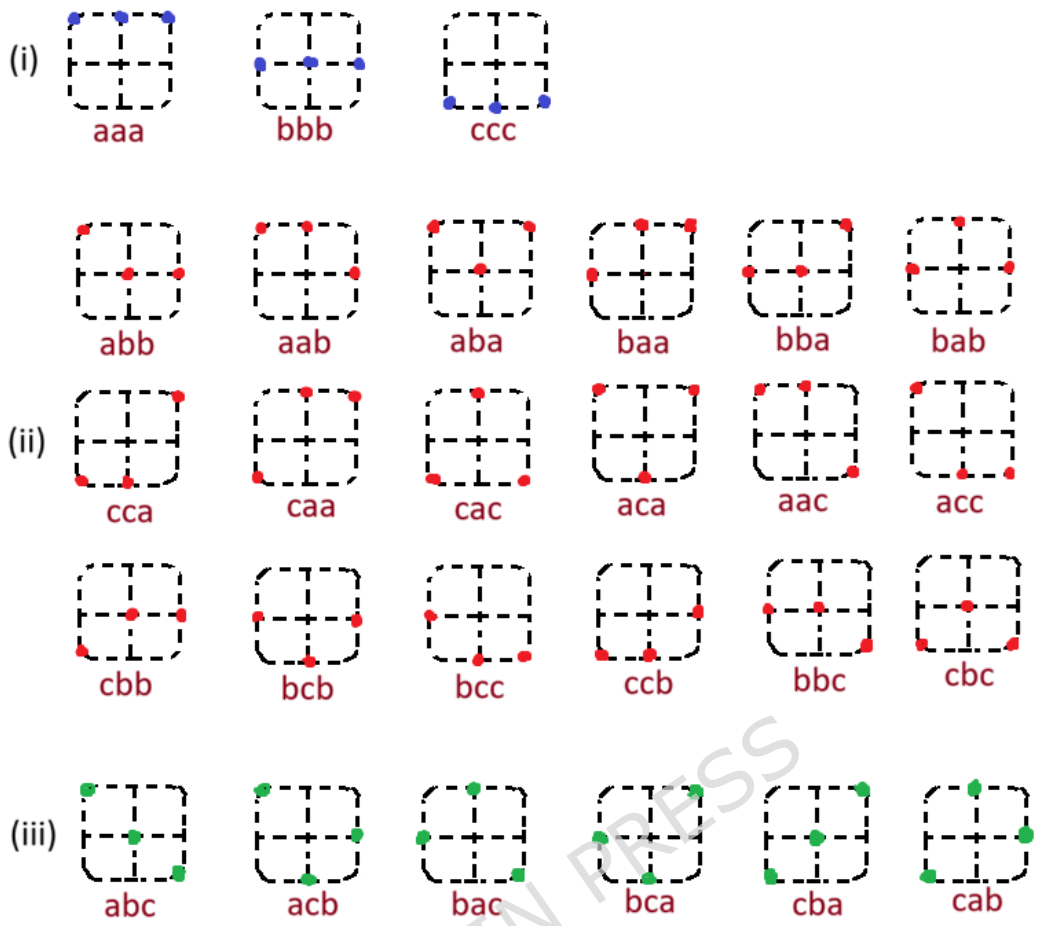

Fig.6. Switching modes of 3-phase direct AC to AC converter (a) Zero modes (ii) Active modes (iii) invert & non-invert modes

The operation of a 3-phase matrix converter involves a total of 27 permissible switching modes, which include 18 active vector modes, 3 zero vector modes, 3 non-invert vector modes, and 3 invert vector modes. The switches are controlled in a rotational manner, ensuring that no two switches in the same leg (i.e., connected to the same output phase) are turned ON simultaneously. This switching strategy maintains safe operation, avoids short circuits, and ensures proper formation of output waveforms through controlled modulation.

In a 3-phase matrix converter, four key types of vector modes active, zero, normal, and inverting—are used to control power flow and synthesize the desired output waveform. Active vector modes occur when each output phase is associated to a different input phase, producing a non-zero output voltage and enabling control of amplitude and frequency; there are 18 such

combinations. Zero vector modes, with all output phases associated to the same input phase (3 modes), generate zero output voltage and are used to reduce switching losses and stabilize modulation. Non-inverting vector modes (3 modes) involve two output phases associated to one input phase and the third to another, supporting smooth transitions between vectors. Similarly, inverting vector modes (3 modes) follow a comparable connection pattern but invert the output vector direction, enhancing modulation flexibility. These vector modes, selected and sequenced through advanced modulation strategies like 3D Space Vector Modulation, enable efficient and reliable AC-AC conversion with high-quality sinusoidal output. These above 4 category of vector modes are utilized in different proportions and sequences depending on the 3D-SVM modulation strategy, to synthesize high-quality sinusoidal waveforms at the output, while ensuring safe and efficient operation of the matrix converter.

4. 3D-Space Vector Modulation

3D-SVM is an advanced modulation technique that extends the concept of traditional space vector modulation by considering all three output phases simultaneously in a 3Dcubic region. The reference vector is tracked in various subcubes and prism to generate the switching pulses for matrix converter. It divides the voltage space into several prisms, each associated with a set of permissible switching states of the matrix converter. Within each switching cycle, the desired output voltage vector is synthesized by computing a weighted combination of active and zero vectors, which are derived based on the state of the nine bidirectional switches. The main advantages of 3D-SVM includes high-quality output waveforms with low harmonic distortion, efficient use of the input voltage, allowing control over both amplitude and frequency, minimized switching losses, and improved performance in hybrid systems by enabling precise power balancing between PV and fuel cell sources. This makes 3D-SVM an

ideal modulation strategy for hybrid renewable systems where dynamic performance, high efficiency, and power quality are critical.

The 3D-SVM operates without redundancy in switching states, where each vertex corresponds to a unique switching state. As a result, the calculation of switching times is simpler compared to conventional SVM. The mathematical design is straightforward, eliminating the need for Park transformations and angle determinations. This approach leads to improved Common Mode Voltage (CMV) mitigation and minimizes capacitor balancing issues when compared to 2D-SVM. In 3D-SVM, switching times are computed without relying on any external parameters or complex calculations.

The following are used to implement and analysis of 3D-SVM

- Identify the subcube to track the reference vector in the 3D-cubic region
- Prism identification to track the reference vector positioned within the subcubes.
- Calculation of the switching times.

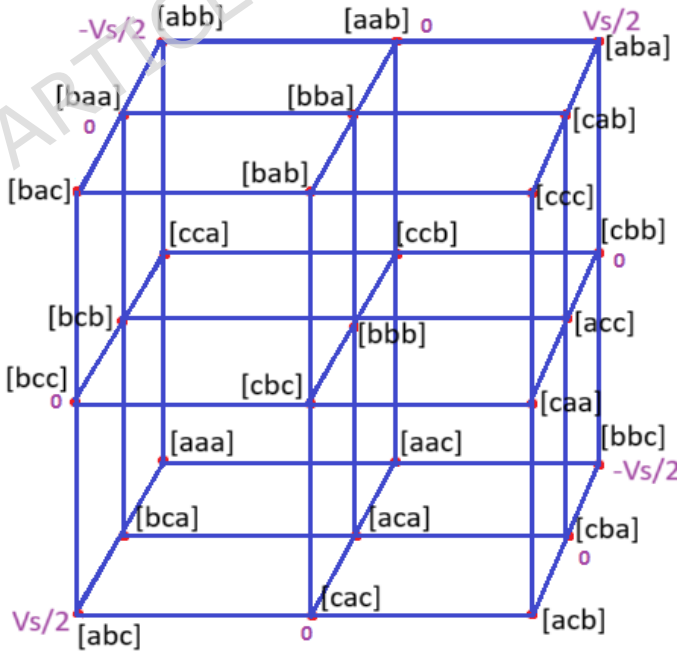

Fig.7. Representation of 3D-SVM with switching modes

In 3D-SVM, the cubic structure is constructed up of eight subcubes, encompassing a total of 27 switching state vectors. Each subcube contains six prisms, and each prism is defined by four switching vectors at its four vertex points. In hybrid systems, matrix converters eliminate the need for a bulky DC-link, enabling compact, efficient AC-AC conversion. The 3D-SVM technique enhances this process by providing precise voltage control, reduced switching losses, improved harmonic performance, and efficient power flow management between the Fuel Cell, PV sources, and the load. The switching pulses are spawned by tracking the reference location within the subcube and prism in the 3D cubic space plane, as illustrated in Fig.7.

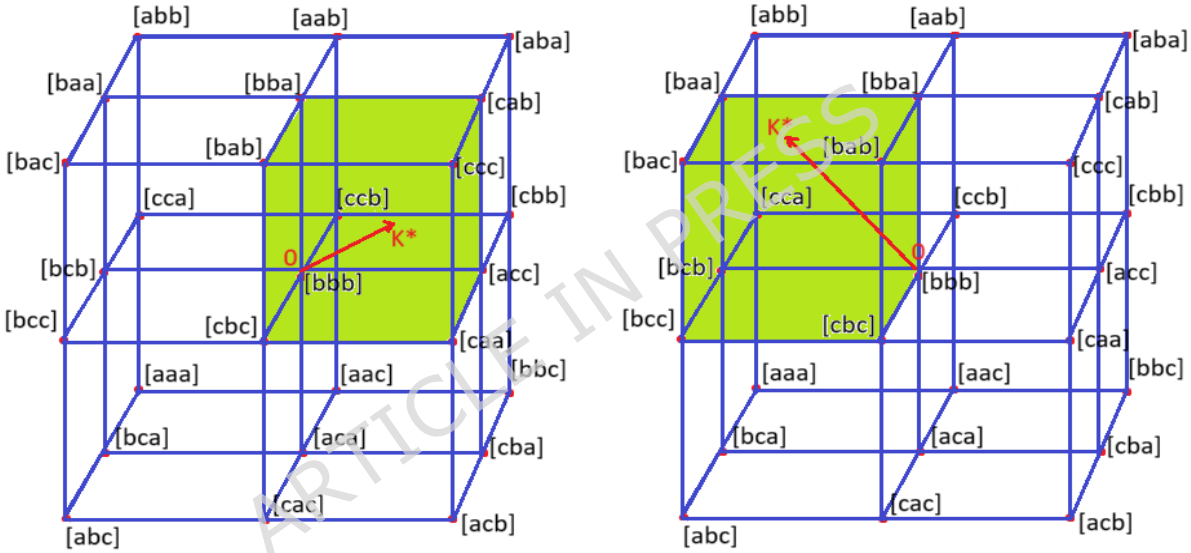

Fig. 8. Depiction & Tracking of various subcubes in 3D Region (a) Subcube 1 (b) Subcube 2

The switching vectors of the 3-phase AC to AC matrix converter are epitomised in a 3D cubic space plane, which is partitioned into 8 subcubes to track the reference vector location, as shown in Fig.8. This subcube space is further disintegrated into 6 prisms to calculate the 4 switching state vectors. For a given normalized reference vector in the three-phase coordinates (X_a, X_b, X_c), the integer part of each component (a, b, c) is computed, where a=integer (X_a); b=integer (X_b); c=integer (X_c).

The 3D cubic space plane is defined by a specific number of subcubes, which depends on the number of levels in the converter. Generally, for an n-level 3-phase converter, the space consists of $(n-1)^3$ subcubes. In the case of the 3-phase matrix converter, there are 8 subcubes. The coordinates (a, b, c) represent the origin of the reference system for the subcube, where the reference vector is directed. In that, two subcubes illustrate to find desired reference voltage vector (K*), is located within a particular subcube formed by switching state vectors. In Subcube 1, the reference vector K* lies within a region bounded by the states [bib], [ccb], and other neighboring vectors. Similarly, in Subcube 2 (b), K* is located within a different subcube region bordered by [bab], [cca], [cbc], etc. Identifying and tracking these subcubes is essential in 3D-SVM as it enables the algorithm to determine the correct set of switching vectors and their corresponding time durations for generating the required output voltage vector with minimal harmonic distortion.

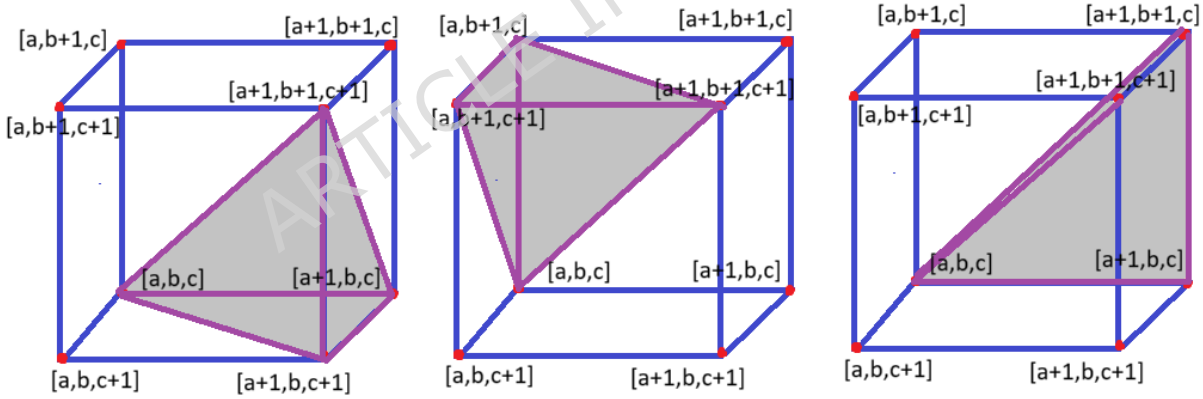

Fig. 9. Depiction & Tracking of various prisms in subcube (a) Prism 1 (b) Prism 2

Each subcube contains six prisms, resulting in a total of 48 prisms in the 3D cubic space plane. To determine the prism in which the reference vector is located, comparisons with three planes in the 3D space are made, defining the six prisms within each subcube. The reference voltage vectors

are then used to assessment the switching states, from which the switching times are derived. After identifying the coordinates (a, b, c), which correspond to the reference system, the subcube diagram is further subdivided into six prisms. Each prism contains four switching state vectors, located at distinct vertex points. The reference vector K* resides within one of these eight volumes of the subcube. The process of locating the reference vector across different prisms is illustrated in Fig.9.

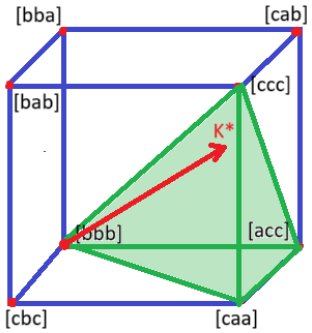

Fig. 10. Switching time calculation for prism 1 using NSV

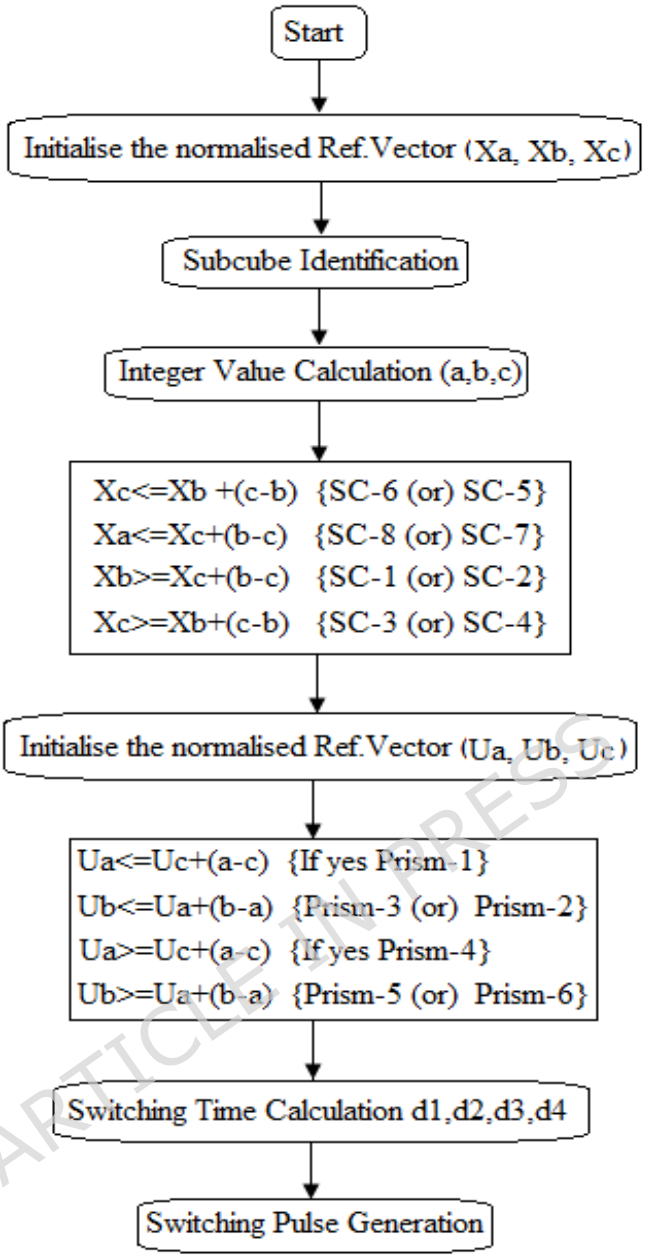

Fig. 11. Flowchart for 3D-SVM implementation

After identifying the prism within various subcubes, the reference voltage vector is accurately established. The switching durations D_1, D_2, D_3 & D_4 are then computed based on prism tracking across these subcubes, utilizing the Nearest State Vector method, which is shown in fig.10. Using the NSV scheme, appropriate switching vectors are selected for each prism based on their ability to minimize THD, CMV, neutral current and improved output voltage. The general expressions for

calculating the gating times corresponding to different prisms are given as follows:

$$d_1 = 1 - \max(v_s) \quad (14)$$

$$d_2 = \max(v_s) - \text{integer}(v_s) \quad (15)$$

$$d_3 = \text{integer}(vs) - \min(v_s) \quad (16)$$

$$d_4 = \min(v_s) \quad (17)$$

Using the above equations, the gating time for each prism within the respective subcubes is determined. Subsequently, the gating pulses for three phase matrix converter are generated based on the calculated switching times. The switching pulses of every prism is generated using subcube identification, prism identification, integer value calculation to track the normalised reference vector and switching times are analysed, the flowchart chart of 3D-SVM implementation is shown in fig.11.

The proposed method employs a rule-based supervisory energy management strategy combined with 3D Space Vector Modulation (3D-SVM) to control a hybrid PV–PEMFC fed three-phase matrix converter. The PV source is treated as the primary energy provider, while the fuel cell operates as a supporting and backup source to ensure continuous power delivery. Based on real-time measurements of PV power availability and load demand, the supervisory controller allocates power references to each source, ensuring smooth power sharing and protecting the fuel cell from rapid transients. These power references are directly integrated into the 3D-SVM algorithm, which optimally selects switching vectors in the three-dimensional cubic space of the matrix converter to achieve low harmonic distortion, reduced common-mode voltage, and stable output voltage. This coordinated control approach enables efficient energy

utilization, improved power quality, and reliable operation of the hybrid energy system.

5. Simulation results and discussions

This section presents the simulation results of the proposed Fuel Cell–Photovoltaic (PV) fed hybrid energy system interfaced with a three-phase matrix converter using 3D-SVM. The performance of the matrix converter under varying operating conditions is evaluated through MATLAB/Simulink simulations. The primary objective is to validate the effective integration of renewable hybrid sources and the ability of the 3D-SVM technique to ensure high-quality power transfer with minimal THD. The simulation parameters are shown in table.2.

Table. 2. Simulation Parameters

Details	Values / Ranges
Solar Radiation	400 - 1000 W/m²
Temperature	40 °C
PV output voltage	92 V
PEMFC Rated power	1 KW
Nominal cell voltage	0.7 V
Rated stack voltage	48 V
Rated current	30 A
Matrix converter Input voltage	230 – 410 V
Input current	10- 30 A
Output power	2 KW

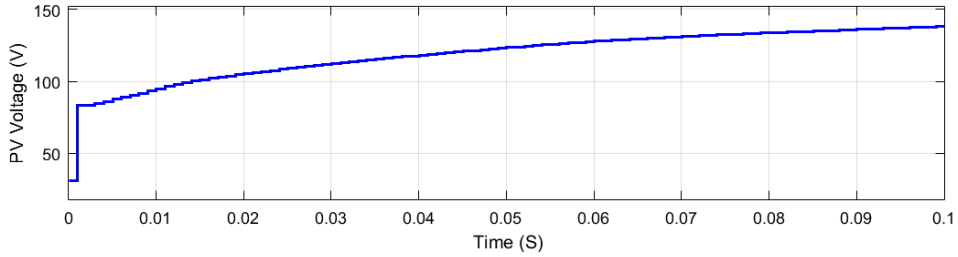

Fig.12. PV system – output DC voltage

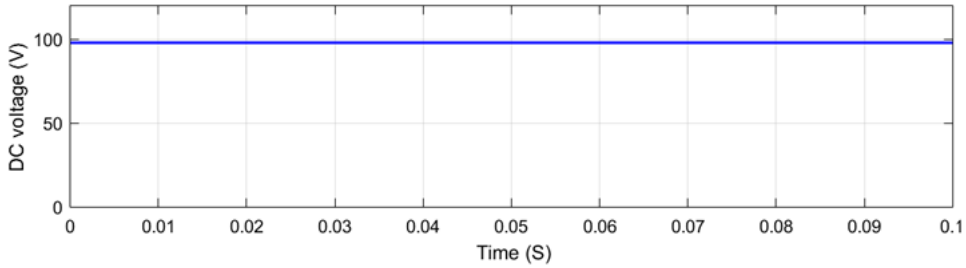

Fig.13. PEMFC – output DC voltage

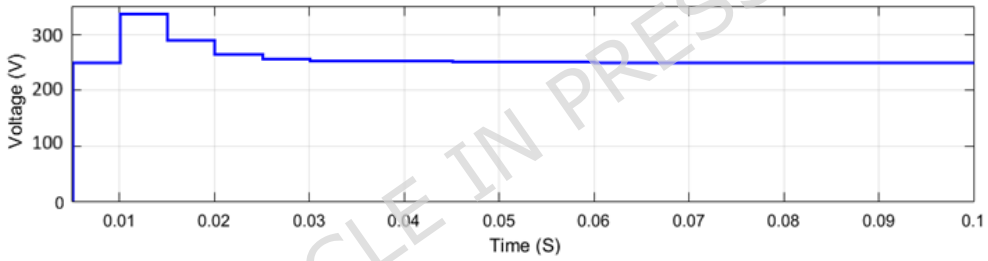

Fig. 14. Hybrid PV - PEMFC output DC voltage

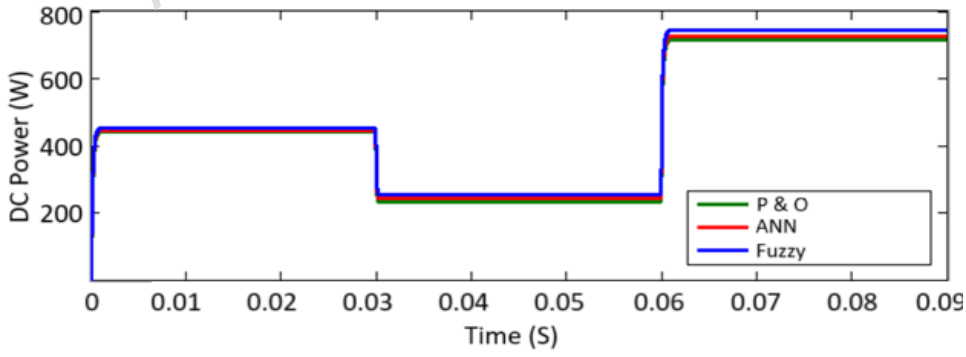

Fig. 15. MPPT controller – comparison for PV output power

The fig.12 shows the photovoltaic system DC output voltage, with voltage 118 V; where solar radiation varies from 400 W/m^2 to 1000 W/m^2 with temperature of 40 °C. PEMFC – output DC voltage is shown in fig.13, with

voltage of 92 V. PEMFC can deliver a constant DC voltage under the given operating conditions without significant fluctuations. This consistent performance is crucial for maintaining reliable input to the matrix converter.

The fig.14 illustrates the comparison of PV output power under different MPPT techniques includes P&O, Artificial Neural Network, and Fuzzy Logic Controller. Among the controllers, the Fuzzy Logic achieves the fastest and most accurate tracking to the new power levels, closely followed by ANN, while the conventional P&O shows slightly slower tracking and minor steady-state oscillations. This comparison highlights that intelligent controllers like Fuzzy and ANN provide improved dynamic response and higher steady-state accuracy compared to traditional P&O methods in rapidly changing environmental conditions. Three phase VSI stepped output voltage is shown in fig.15, with voltage of 210 V. The fig.16 shows the switching pulses generated for the 9 bidirectional switches of the three-phase matrix converter using 3D-SVM technique; The pulses demonstrate a highly structured and coordinated switching sequence, ensuring that at every instant, two switches are ON to maintain the required three-phase output.

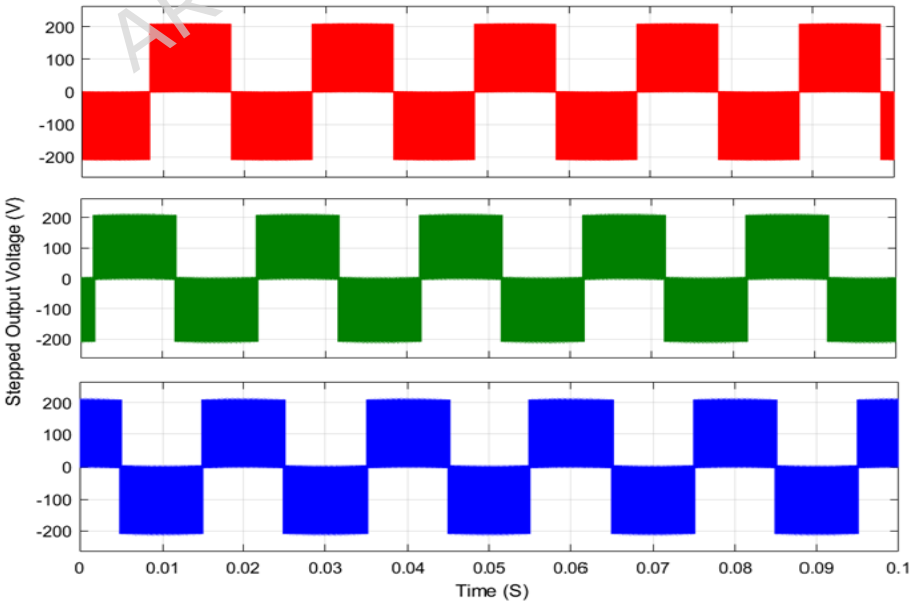

Fig.16. Stepped output voltage of 3-phase VSI

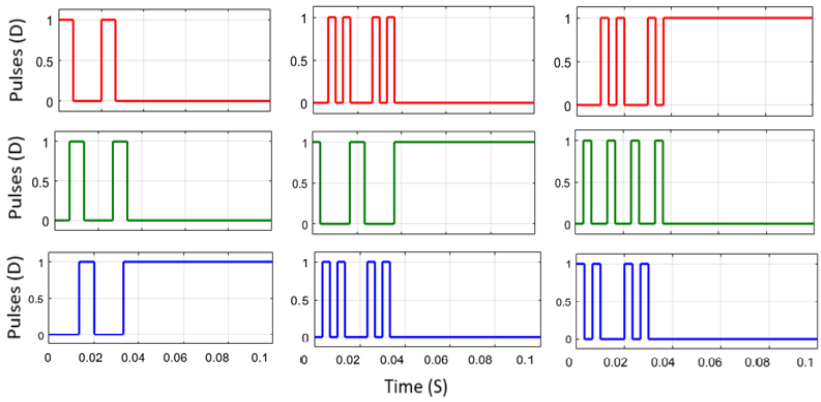

Fig.17. Switching pulses for 3-phase matrix converter using 3D-SVM

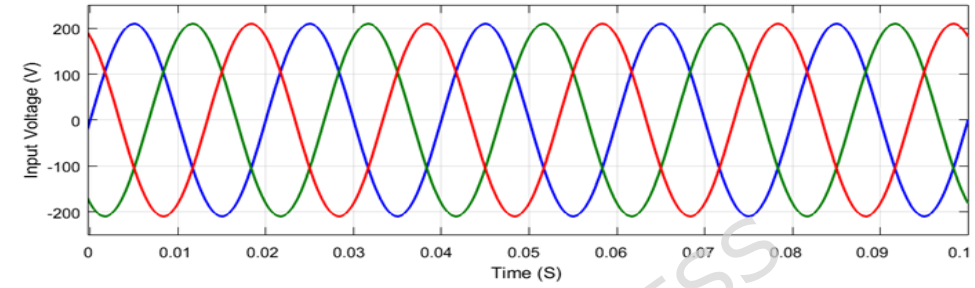

(a)

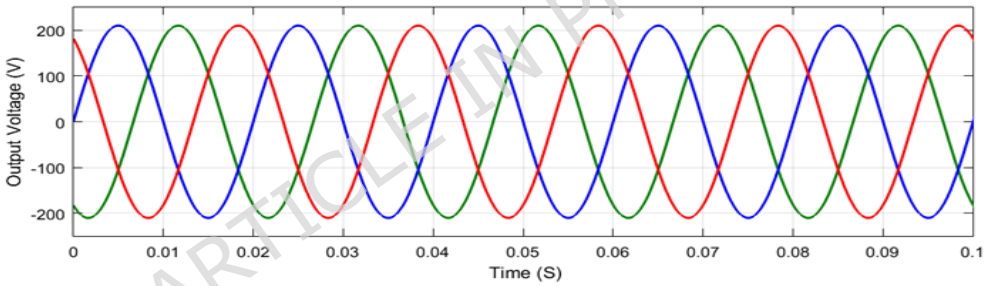

(b)

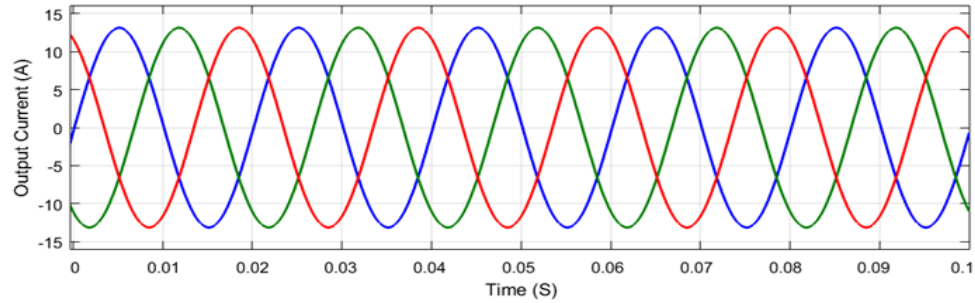

(c)

Fig.18. 3-phase direct AC-AC matrix converter (a) input voltage (b) output voltage (c) output current

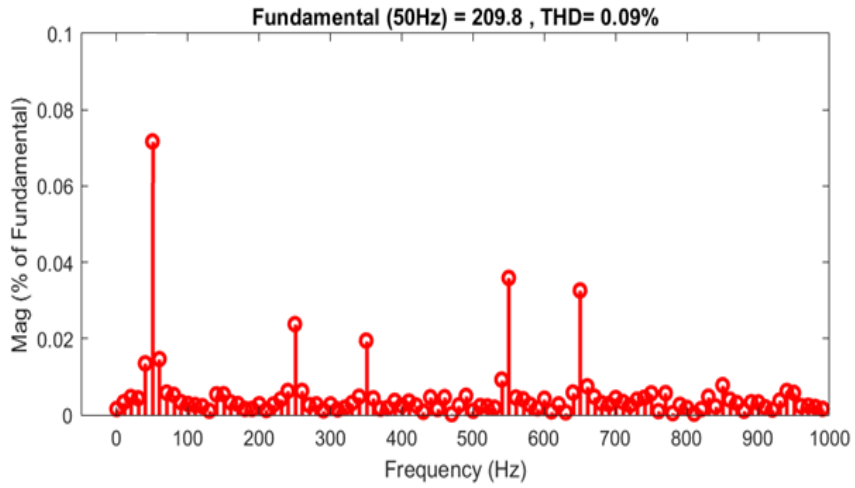

(a)

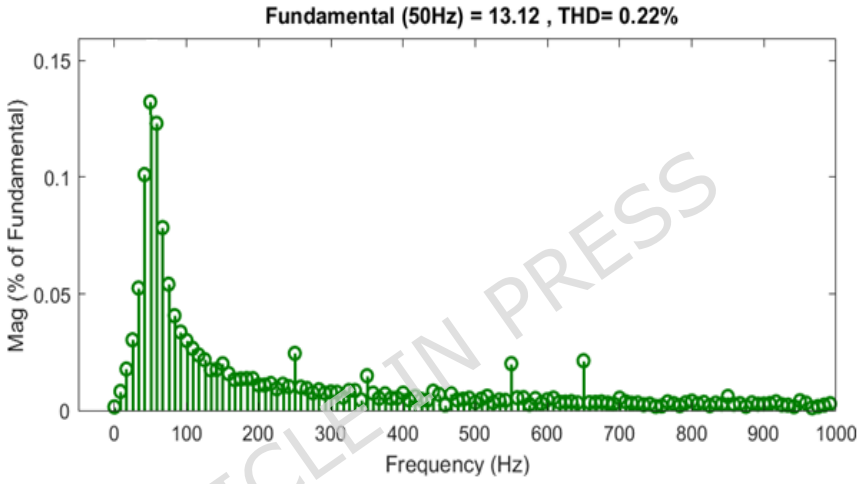

(b)

Fig.19. THD analysis for matrix converter (a) voltage (b) current

The fig.18 illustrates the performance of a three-phase direct AC-AC matrix converter operating under (3D-SVM control.; in that fig.18a shows the applied AC input voltage with value of 210 V, and fig.18b shows the AC output voltage of matrix converter with voltage of 209.8 V; and fig.18c shows the output current of matrix converter, which is balanced, sinusoidal, & properly aligned with their respective output voltages, indicating effective load power delivery and efficient operation.

The smoothness and symmetry in the current waveforms confirm minimal harmonic distortion of the proposed system. The fig.19 shows the THD analysis of proposed system; in that fig.19a shows the THD for output

voltage spectrum with fundamental component at 50 Hz with a magnitude of 209.8 V and THD of 0.09%, confirming that the voltage is nearly sinusoidal with minimal harmonic distortion. Similarly, in fig.19b presents the output current spectrum with the fundamental at 50 Hz and a magnitude of 13.12 A, with THD of 0.22%. These results validate that the 3D-SVM strategy effectively controls the matrix converter, delivering high-quality output with very low harmonic content.

6. Hardware results and discussion

The proposed Fuel Cell–PV fed hybrid energy source driving a three-phase Matrix Converter using 3D-Space Vector Modulation was experimentally validated through a laboratory prototype consisting of a fuel cell emulator, PV emulator, hybrid energy management system, and a matrix converter built with IGBTs and real-time control implementation using a DSP. Under steady-state operation, the converter maintained a stable three-phase 50 Hz output with high efficiency. Power sharing between the PV and fuel cell was effectively managed, with the PV contributing about maximum of the load demand under normal conditions and the fuel cell compensating during irradiance drops, ensuring uninterrupted supply. The results validate that the proposed system offers high-quality AC output, efficient renewable hybridization, and superior dynamic response, making it a promising solution for AC load applications.

The fig.20 shows the experimental results of the proposed input sources; in that fig.20a shows the PV system DC output voltage with 118 V and fig.20b shows the PEMFC DC output voltage with 90.5 V. The fig.21 shows the three phase VSI stepped output voltage with values of 207.5 V. The switching pulses for 3-phase matrix converter generated using 3D-SVM with help of DSP processor, which is shown in fig.22, for the switches S11, S12 & S13, and similarly switching pulses are generated for other switches of matrix converter.

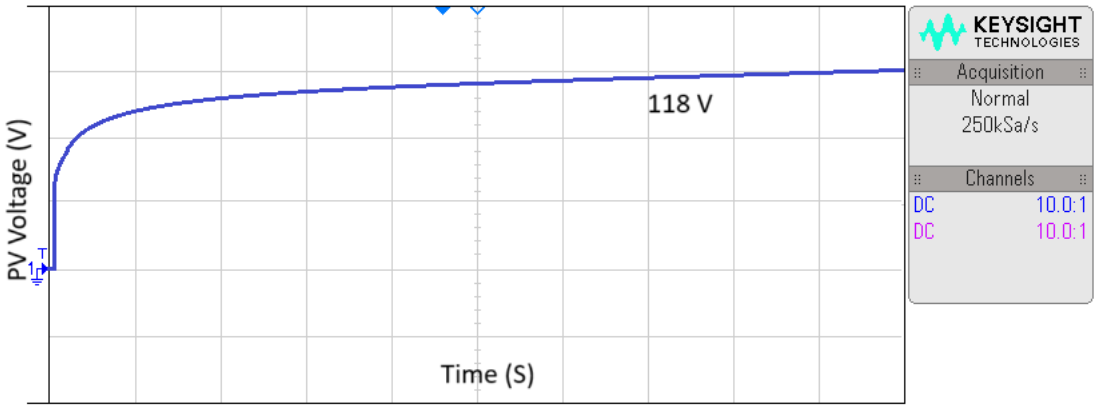

(a)

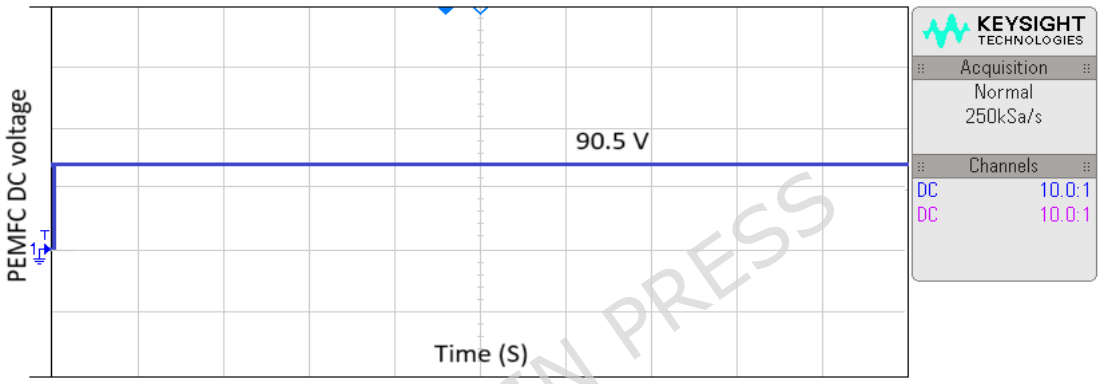

(b)

Fig.20. Experimental results – DC output voltage (a) PV (b) PEMFC

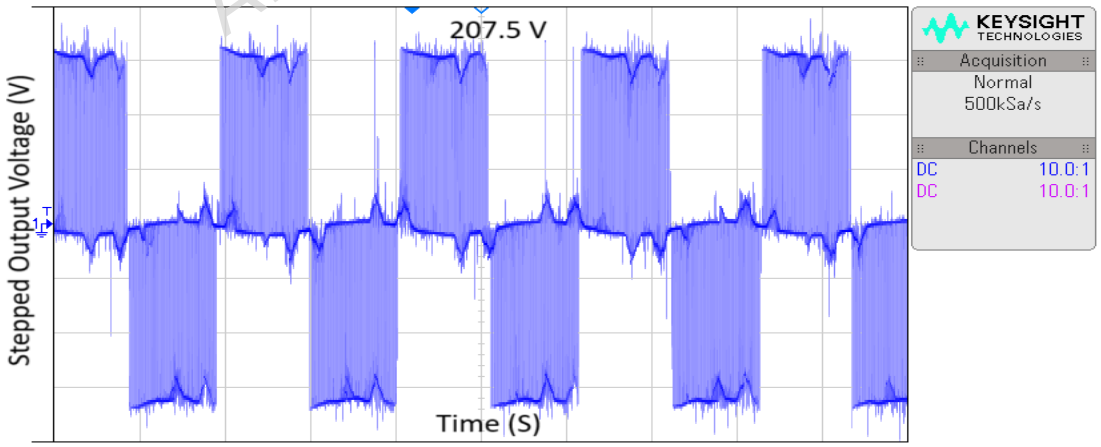

Fig.21. 3-phase VSI – stepped voltage

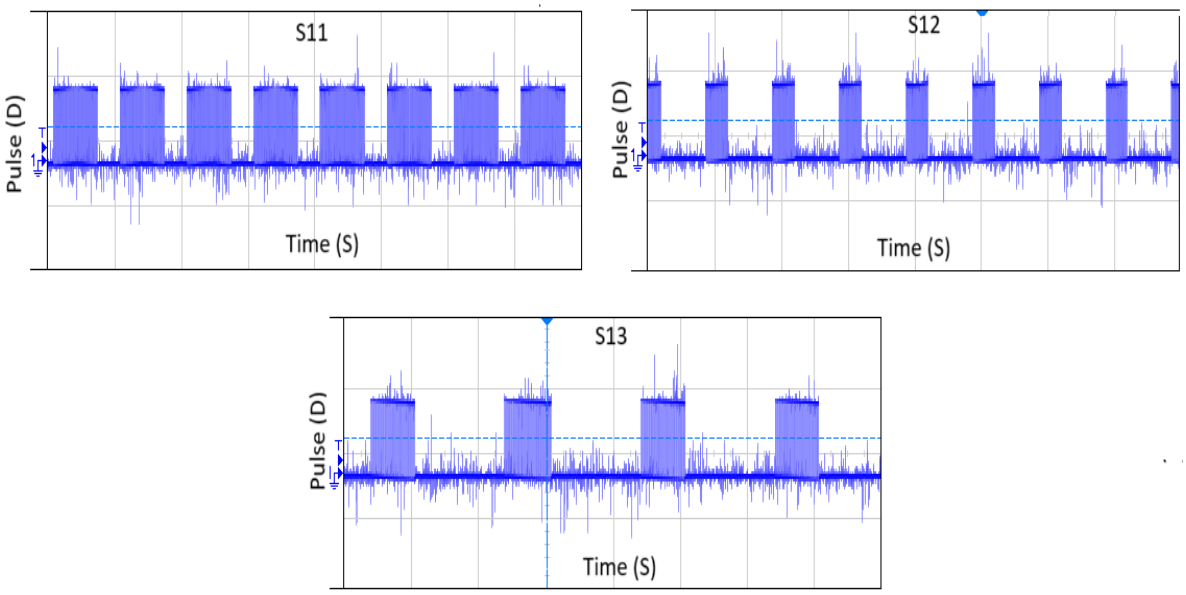

Fig.22. Switching pulses for S11, S12 & S13 switches using 3D-SVM

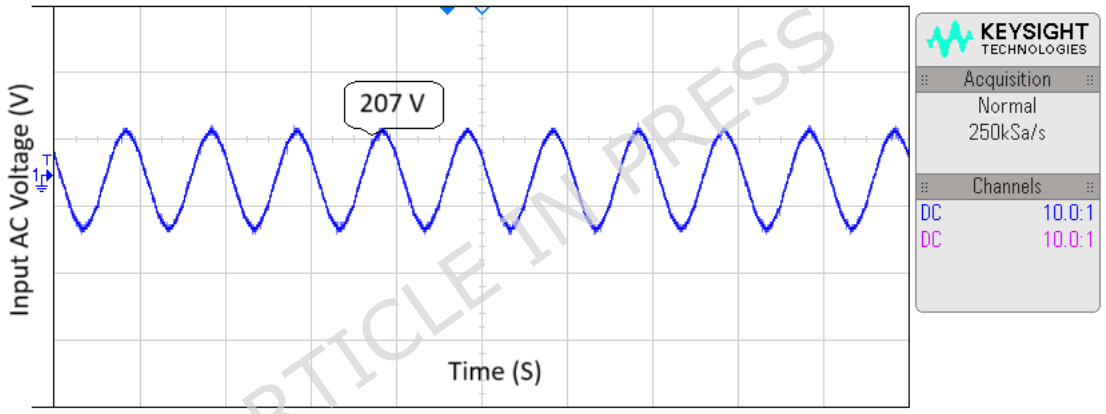

(a)

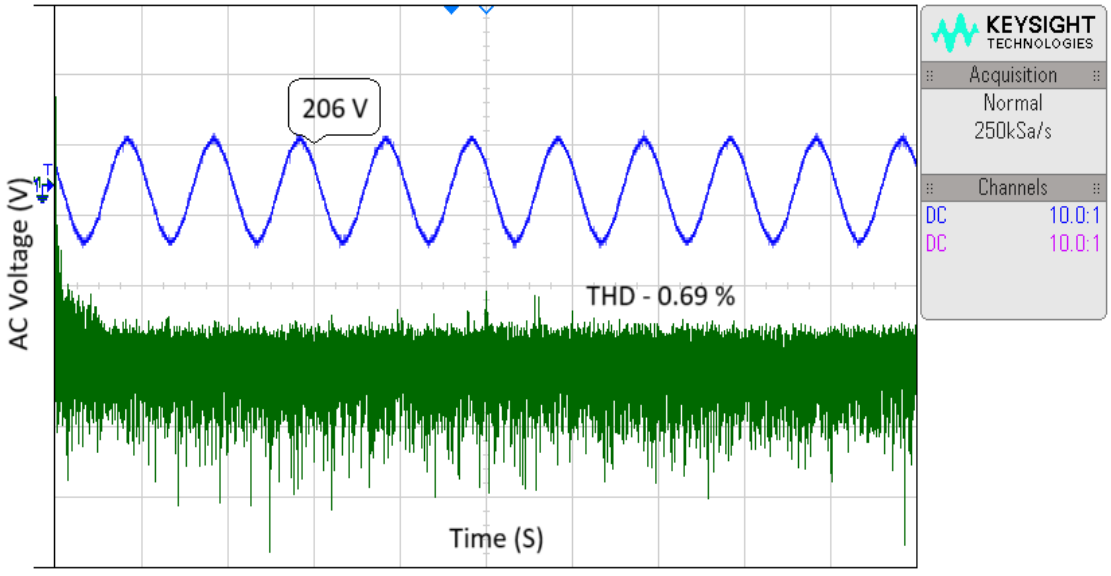

(b)

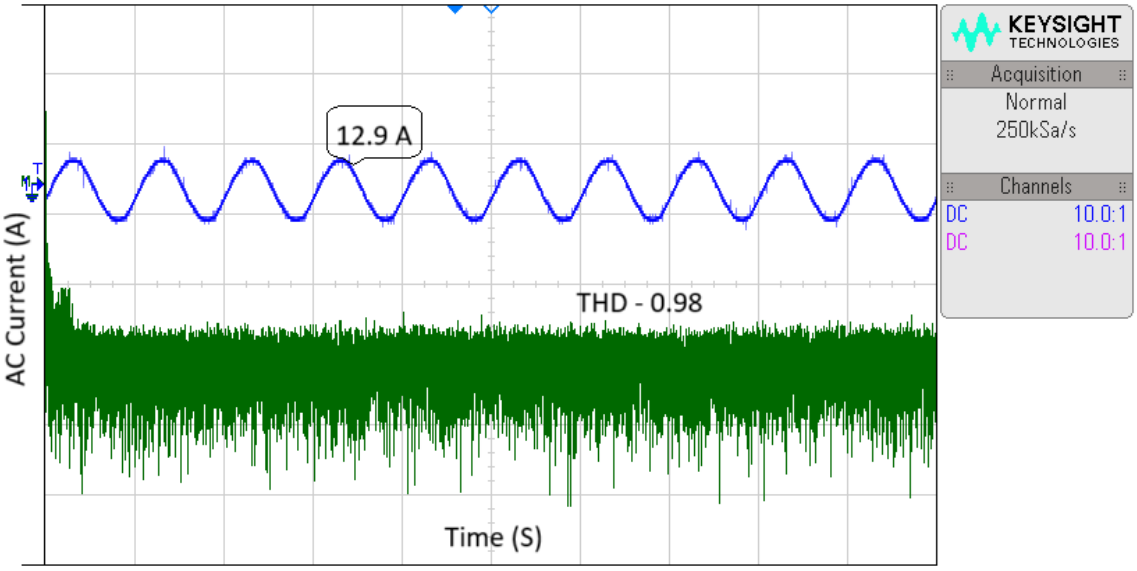

(c)

Fig.23. Experimental results of matrix converter (a) Input voltage (b) Output voltage (c) Output current

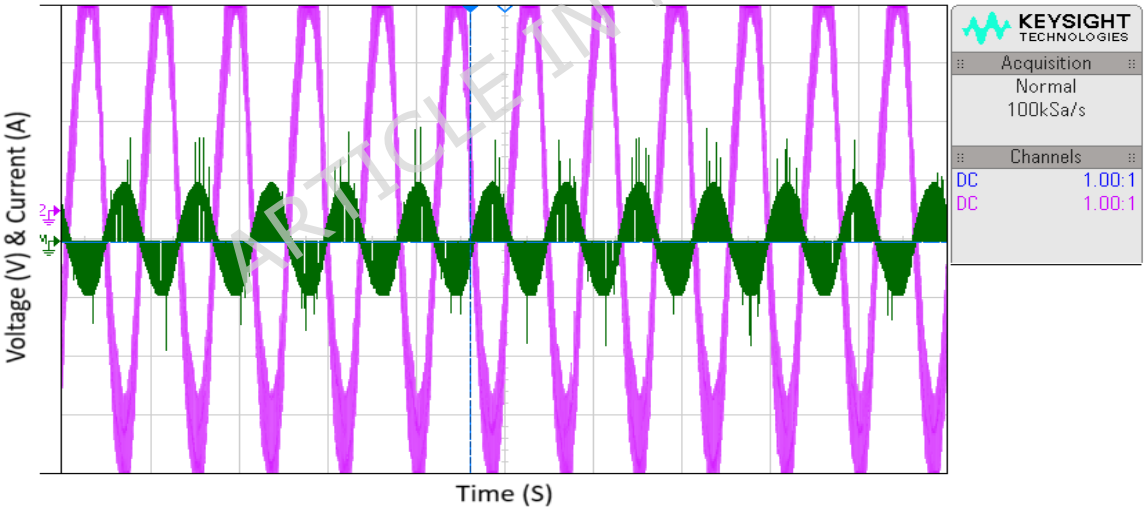

Fig.24. Comparison of matrix converter output voltage & current for Phase-A

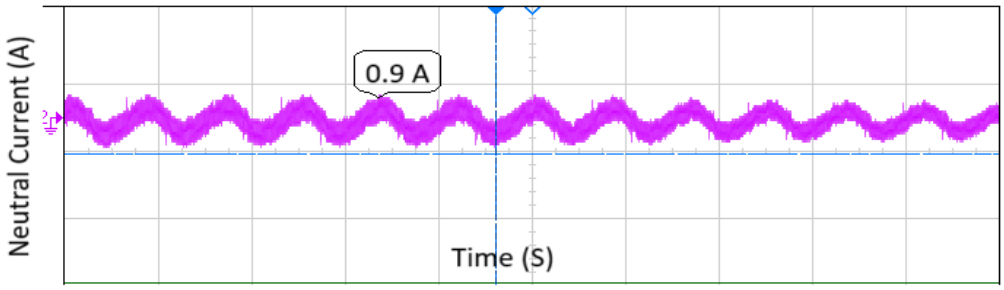

Fig.25. Neutral current of matrix converter

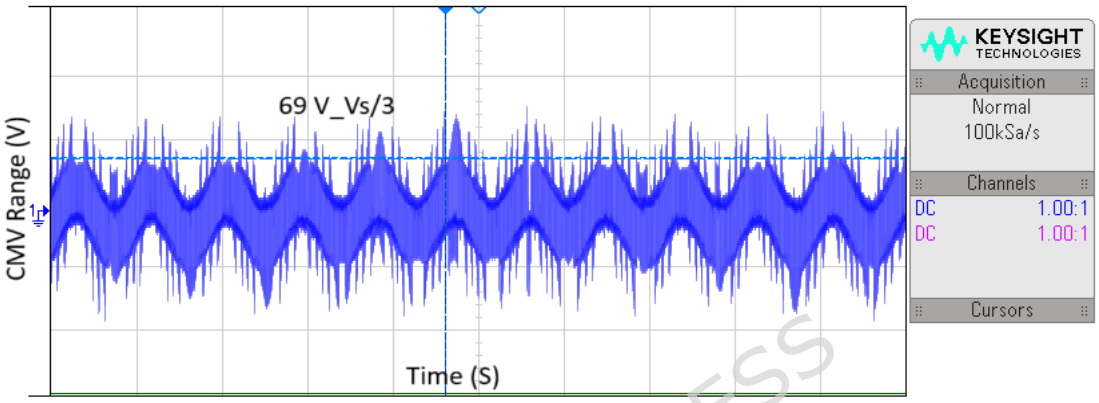

(a)

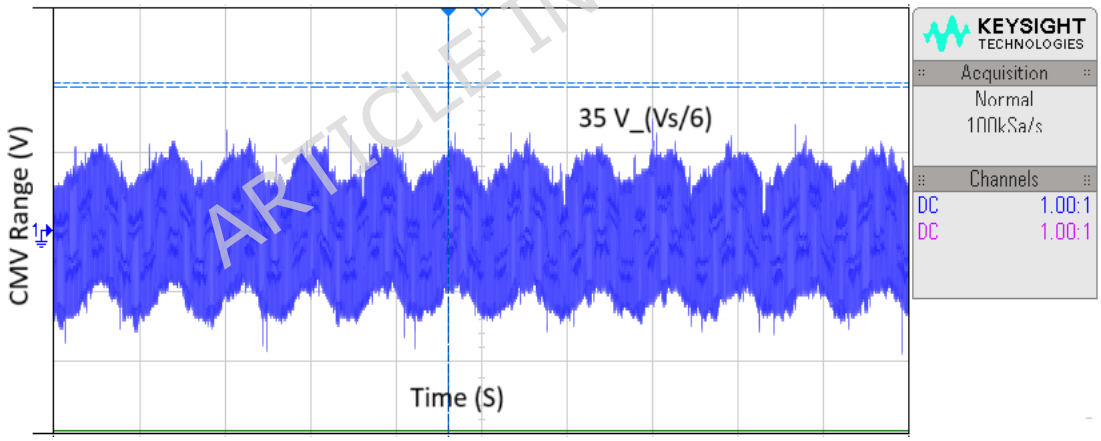

(b)

Fig.26. CMV range (a) 2D-SVM (b) 3D-SVM

Fig.27. Experimental Setup for proposed system

The experimental results of 3-phase direct AC-AC matrix converter is shown in fig.23. In that fig.23a shows the three phase input voltage, which is generated using hybrid energy sources with PV-PEMFC energy source with voltage of 207 V; and fig.23b shows three phase AC output voltage of matrix converter with voltage of 206 V and THD of 0.69%; and the fig.23c shows the AC output current of matrix converter with current of 12.9 A and THD of 0.98%. Fig.24 illustrates a comparison of the matrix converter's output voltage and current for Phase-A. Meanwhile, Fig.25 presents the neutral current of the matrix converter, which is measured at 0.9 A, demonstrating a more effective minimization compared to conventional PWM methods.

The CMV is one of the major drawback in power converters, where the excessive CMV can lead to equipment malfunction, signal interference, increased electromagnetic emissions, and potential safety hazards. In sensitive applications like motor drives, communication systems, and medical equipment, high CMV can cause insulation stress, data errors, and even premature device failure. Effective CMV minimization improves system reliability, enhances performance, reduces EMI, and extends the

lifespan of components. The CMV of the proposed 3-phase matrix converter is depicted in Fig.26. Fig.26a illustrates the CMV reduction achieved using 2D-SVM with a voltage of 69 V, which is Vs/3 of the applied input voltage. In contrast, Fig.26b shows the CMV reduction achieved with 3D-SVM, with a voltage of 35 V, which is one-sixth (Vs/6) of the applied input voltage. The hardware setup for the proposed system is obtainable in Fig.27.

Table.3. Comparison of PWM methods for Neutral current, CMV, and THD reduction

PWM methods	Neutral Current (A)	CMV level	THD reduction	
			Voltage THD (%)	Current THD (%)
SPWM	2.06	142 V (Vdc/2)	2.76 %	3.26 %
MSPWM	1.94	142 V (Vdc/2)	2.48 %	2.86 %
HSVM	1.56	71 V (Vdc/3)	1.20 %	1.46 %
2D SVM	1.15	35 V (Vdc/6)	0.92 %	0.88 %
3D SVM	0.9	35 V (Vdc/6)	0.09 %	0.22 %

Conclusion

This paper successfully demonstrated the integration of a hybrid energy system combining PEMFC and Photovoltaic sources to feed a three-phase matrix converter controlled by a 3D Space Vector Modulation strategy. The hybrid configuration effectively addressed the challenges of power intermittency and dynamic response limitations associated with individual

sources, ensuring a stable and reliable power supply. The implementation of 3D-SVM enabled improved voltage transfer ratio, minimized THD, reduced CMV, lower neutral current, and enhanced dynamic performance of the matrix converter. Simulation and experimental results confirmed the effectiveness and robustness of the proposed system, confirming its potential for advanced renewable energy applications and efficient real-time power management for various AC load applications. The highlight of the manuscript includes:

- Implemented hybrid energy system combining PEMFC and PV sources to feed a three-phase matrix converter using 3D-SVM.
- THD of proposed system is diminished to 0.09% for voltage and 0.22 % for current.
- Neutral current of 3-phase matrix converter is reduced to 0.9 A.
- The CMV is minimized to 35 V, which is less than Vs/6 times of applied AC input voltage.

Future Scope: Future research can include dynamic load testing, integration of small energy-storage support, and advanced supervisory control for improved power sharing. Real-time implementation using DSP/FPGA platforms, scalability to higher-power or grid-connected systems, and reliability/thermal assessment of the matrix converter can further strengthen the practical applicability of the proposed hybrid FC–PV system.

Data availability: The datasets used and/or analysed during the current study available from the corresponding author on reasonable request.

Acknowledgment: The authors extend their appreciation to the Deanship of Research and Graduate Studies at King Khalid University for funding this work through Large Research Project under grant number RGP 2/173/45. This research work is supported by the Ministry of Higher Education (MOHE) under the 2023 Translational Research Program for the Energy Sustainability Focus Area (Project ID: MMUE/240001), the

2024 ASEAN IVO (Project ID: 2024-02), and Multimedia University, Malaysia.

References

1. H. HassanzadehFard, F. Tooryan, E. R. Collins, S. Jin, and B. Ramezani, ‘‘Design and optimum energy management of a hybrid renewable energy system based on efficient various hydrogen production,’’ Int. J. Hydrogen Energy, vol. 45, no. 55, pp. 30113–30128, Nov. 2020.
2. M. Xie, M. M. Gulzar, H. Tehreem, M. Y. Javed, and S. T. H. Rizvi, ‘‘Automatic voltage regulation of grid connected photovoltaic system using Lyapunov based sliding mode controller: A finite—Time approach,’’ Int. J. Control, Autom. Syst., vol. 18, no. 6, pp. 1550–1560, Jun. 2020.
3. F. U. Khan, M. M. Gulzar, D. Sibtain, H. M. Usman, and A. Hayat, ‘‘Variable step size fractional incremental conductance for MPPT under changing atmospheric conditions,’’ Int. J. Numer. Model., Electron. Netw., Devices Fields, vol. 33, no. 6, p. e2765, Nov. 2020.
4. G. Anusha, A. Sudhakar, S. Rafikiran, R. R. Deshmukh and C. H. Basha, "Modeling of a Fuel Cell with Boost Converter Using Artificial Neural Network," *2025 International Conference on Visual Analytics and Data Visualization (ICVADV)*, Tirunelveli, India, 2025, pp. 683-690, doi: 10.1109/ICVADV63329.2025.10961057.
5. M. M. Gulzar, D. Sibtain, A. F. Murtaza, S. Murawwat, M. Saadi, and A. Jameel, ‘‘Adaptive fuzzy based optimized proportional-integral controller to mitigate the frequency oscillation of multi-area photovoltaic thermal system,’’ Int. Trans. Electr. Energy Syst., vol. 31, no. 1, 2021, Art. no. e12643.
6. Sreedhar, G., Basha, C.H.H., Likhitha, R., Rafikiran, S., Alsaif, F. (2025). A Novel Analysis of DC-DC Voltage Conversion Circuit with Modified RBFN Controller for Hydrogen Vehicle Technology. In: Bansal, J.C., Jamwal, P., Hussain, S. (eds) Proceedings of the International Conference on AI and Robotics. AIR 2025. Lecture Notes in Networks and Systems, vol 1629.

7. A. Serpi, M. Porru, and A. Damiano, “An optimal power and energy management by hybrid energy storage systems in microgrids,” Energies, vol. 10, no. 11, p. 1909, 2017.
8. C. Y. Wang and L. Wan, “Type-2 fuzzy implications and fuzzy valued approximation reasoning,” Int. J. Approx. Reasoning, vol. 102, pp. 108–122, Nov. 2018.
9. S. V. Krishna, C. Hussaian Basha, B. Sahoo, M. M. Irfan and S. Rafikiran, "A Novel Modelling of Fuel Cell under Different Operational Conditions," *2025 International Conference on Computing Technologies (ICOCT)*, Bengaluru, India, 2025, pp. 1-8, doi: 10.1109/ICOCT64433.2025.11118885.
10. D. Shahzad, S. Pervaiz, N. A. Zaffar, and K K. Afridi, “GaN-Based high-power-density AC–DC–AC converter for single-phase transformerless online uninterruptible power supply,” IEEE Trans. Power Electron., vol. 36, no. 12, pp. 13968–13984, Dec. 2021.
11. Karthikeyan, B., Sundararaju, K. & Palanisamy, R. ANN-Based MPPT Controller for PEM Fuel Cell Energized Interleaved Resonant PWM High Step Up DC-DC Converter with SVPWM Inverter Fed Induction Motor Drive. Iran J Sci Technol Trans Electr Eng (2021). https://doi.org/10.1007/s40998-021-00413-0.
12. M A. Waghmare, B. S. Umre, M V. Aware, A. Kumar, and S A. Yerkal, “Common-mode voltage minimization in three-phase to Sixphase indirect matrix converter using virtual vector synthesization,” IEEE Trans. Ind. Appl., vol. 58, no. 4, pp. 4848–4858, Jul./Aug. 2022.
13. T. N. Mir, B. Singh, and A. H. Bhat, “Single-phase to three-phase matrix converter fed induction motor drive for low speed applications,” in Proc. IEEE Int. Conf. Power Electron., Drives Energy Syst., 2020, pp. 1–6.
14. V. Velu, N. Mariun, M. Amran, and N. Farzilah, “Realization of single phase to three phase matrix converter using SVPWM algorithm,” Automatika: Casopis Za Automatiku, Mjerenje, Elektroniku, Ra˘ ˘ cunarstvo i Komunikacije, vol. 57, no. 1, pp. 129–140, 2016.

15. W. Deng, “Maximum voltage transfer ratio of matrix converter under DTC with rotating vectors,” IEEE Trans. Power Electron., vol. 36, no. 6, pp. 6137–6141, Jun. 2020.
16. S. V. Krishna, C. H. Basha, B. Sahoo and S. Rafikiran, "A Novel Development of ANN-fed Fuel Cell for Hybrid Electric Vehicles," *2025 International Conference on Computing Technologies & Data Communication (ICCTDC)*, HASSAN, India, 2025, pp. 1-6, doi: 10.1109/ICCTDC64446.2025.11158776.
17. D. Cao, S. Jiang, and F. Z. Peng, “Optimal design of a multilevel modular capacitor-clamped DC–DC converter,” IEEE Trans. Power Electron., vol. 28, no. 8, pp. 3816–3826, Aug. 2013.
18. R. Palanisamy, V. Shanmugasundaram, S. Vidyasagar and K. Vijayakumar, “A Comparative Analysis of Hysteresis Current Control SVM and 3D-SVM for 3-Level NPC Inverter”, Journal of Circuits, Systems and Computers, Vol. 31, No. 2 (2022), 2230002.
19. T. N. Mir, B. Singh, and A. H. Bhat, “Investigation on operational range and suitable control for single phase to three phase matrix converter,” in Proc. IEEE Energy Convers. Congr. Expo., 2021, pp. 2402–2407.
20. M. A. Waghmare, B. S. Umre, M. V. Aware, A. Iqbal, and A. Kumar, “Dual stage single-phase to multiphase matrix converter for variable frequency applications,” IEEE Trans. Power Electron., vol. 38, no. 2, pp. 1372–1377, Feb. 2023.
21. X. Li, Y. Sun, L. Jiang, S. Xie, Y. Liu, and M. Su, “A Modulation scheme to reduce leakage current of split-capacitor four-wire current source inverter,” IEEE Trans. Power Electron., vol. 38, no. 10, pp. 13156–13165, Oct. 2023.
22. X. Guo, S. Du, N. Diao, C. Hua, and F. Blaabjerg, “Three-dimensional space vector modulation for four-leg current-source inverters,” IEEE Trans. Power Electron., vol. 38, no. 10, pp. 13122–13132, Oct. 2023.
23. G. Tan, J. Wei, W. Zhao, L. Qi, and X. Sun, “Application of threedimensional unbalanced coordinate transformation to stand-alone

fourleg voltage-source inverter," IEEE Trans. Power Electron, vol. 37, no. 10, pp. 11686–11703, Oct. 2022.

24. Q. Yan, Z. Zhou, M. Wu, X. Yuan, R. Zhao, and H. Xu, "A simplified analytical algorithm in abc coordinate for the three-level SVPWM," IEEE Trans. Power Electron., vol. 36, no. 4, pp. 3622–3627, Apr. 2021.
25. L. Xu and Z. Q. Zhu, "A novel SVPWM for open winding permanent magnet synchronous machine with extended operation range," IEEE J. Emerg. Sel. Topics Power Electron., vol. 11, no. 1, pp. 901–914, Feb. 2023.
26. Z. Dong and C. Liu, "Three-dimension space vector modulation for three-phase series-end winding voltage-source inverters," IEEE Trans. Ind. Electron., vol. 71, no. 1, pp. 82–92, Jan. 2024.
27. C. Sun, D. Sun, Z. Zheng, and H. Nian, "Simplified model predictive control for dual inverter-fed open-winding permanent magnet synchronous motor," IEEE Trans. Energy Convers., vol. 33, no. 4, pp. 1846–1854, Dec. 2018.
28. M. Maaruf, K. Khan, and M. Khalid, ''Robust control for optimized islanded and grid-connected operation of solar/wind/battery hybrid energy,'' Sustainability, vol. 14, no. 9, p. 5673, May 2022.
29. Y. Alhumaid, K. Khan, F. Alismail, and M. Khalid, ''Multi-input nonlinear programming based deterministic optimization framework for evaluating microgrids with optimal renewable-storage energy mix,'' Sustainability, vol. 13, no. 11, p. 5878, May 2021.
30. Y. Ma, C. Li, and S. Wang, ''Multi-objective energy management strategy for fuel cell hybrid electric vehicle based on stochastic model predictive control,'' ISA Trans., vol. 131, pp. 178–196, Dec. 2022.